

AperTO - Archivio Istituzionale Open Access dell'Università di Torino

**Risk stratification of patients with SARS-CoV-2 by tissue factor expression in circulating extracellular vesicles**

**This is a pre print version of the following article:**

*Original Citation:*

*Availability:*

This version is available <http://hdl.handle.net/2318/1863581> since 2022-06-06T17:31:49Z

*Published version:*

DOI:10.1016/j.vph.2022.106999

*Terms of use:*

Open Access

Anyone can freely access the full text of works made available as "Open Access". Works made available under a Creative Commons license can be used according to the terms and conditions of said license. Use of all other works requires consent of the right holder (author or publisher) if not exempted from copyright protection by the applicable law.

(Article begins on next page)

1 **Risk stratification of patients with SARS-CoV-2 by tissue factor expression in**  
2 **circulating extracellular vesicles**

3 Jacopo Burrello<sup>a,b</sup>; Elena Caporali<sup>c</sup>; Lorenzo Grazioli Gauthier<sup>d</sup>; Enea Pianezzi<sup>e</sup>; Carolina  
4 Balbi<sup>f,g</sup>; Elia Rigamonti<sup>d</sup>; Sara Bolis<sup>a,f</sup>; Edoardo Lazzarini<sup>a</sup>; Vanessa Biemmi<sup>a</sup>; Alessio  
5 Burrello<sup>h</sup>; Roberto Frigerio<sup>i</sup>; Gladys Martinetti<sup>e</sup>; Tanja Fusi-Schmidhauser<sup>d</sup>; Giuseppe  
6 Vassalli<sup>f,g,i</sup>; Enrico Ferrari<sup>c</sup>; Tiziano Moccetti<sup>c</sup>; Alessandro Gori<sup>i</sup>; Marina Cretich<sup>i</sup>; Giorgia  
7 Melli<sup>l,m</sup>; Silvia Monticone<sup>b</sup>; Lucio Barile<sup>a,l,n</sup>.

8

9 <sup>a</sup> Laboratory for Cardiovascular Theranostics, Istituto Cardiocentro Ticino, Ente Ospedaliero  
10 Cantonale Lugano, Switzerland; <sup>b</sup> Division of Internal Medicine and Hypertension Unit,  
11 Department of Medical Sciences, University of Torino, Italy; <sup>c</sup> Cardiology Department,  
12 Istituto Cardiocentro Ticino, Ente Ospedaliero Cantonale, Lugano, Switzerland; <sup>d</sup> Internal  
13 Medicine Department, Ospedale Regionale di Lugano, Ente Ospedaliero Cantonale,  
14 Lugano, Switzerland; <sup>e</sup> Laboratory of Microbiology, Ente Ospedaliero Cantonale, Bellinzona,  
15 Switzerland; <sup>f</sup> Laboratory of Cellular and Molecular Cardiology, Istituto Cardiocentro Ticino,  
16 Ente Ospedaliero Cantonale, Lugano, Switzerland; <sup>g</sup> Center for Molecular Cardiology,  
17 Zürich, Switzerland; <sup>h</sup> Department of Electrical, Electronic and Information Engineering  
18 (DEI), University of Bologna, Bologna, Italy; <sup>i</sup> Istituto di Scienze e Tecnologie Chimiche  
19 "Giulio Natta" (SCITEC), Consiglio Nazionale delle Ricerche, Milano, Italy; <sup>l</sup> Faculty of  
20 Biomedical Sciences, Università della Svizzera italiana, Lugano, Switzerland; <sup>m</sup> Laboratory  
21 for Biomedical Neurosciences, Neurocenter of Southern Switzerland, Lugano, Switzerland;  
22 <sup>n</sup> Institute of Life Science, Scuola Superiore Sant'Anna, Pisa, Italy.

23

24 *Running title:* CD142-EV to predict prognosis in SARS-CoV2

25

26 *Corresponding author:* Lucio Barile, PhD, Cardiocentro Ticino Institute, Ente Ospedaliero  
27 Cantonale, Via Tesserete 48, 6900 Lugano, Switzerland (+41 910586667104).

28 E-mail: [lucio.barile@eoc.ch](mailto:lucio.barile@eoc.ch) / [lucio.barile@usi.ch](mailto:lucio.barile@usi.ch)

29

30 Manuscript word count: 5,564 words including title, abstract, and references.

31 Abstract word count: 230.

32 Number of Tables: 1; Number of Figures: 4; 1 Supplemental file (5 Figures; 13 Tables).

33 Reference count: 32.

34 **ABSTRACT**

35 Inflammatory response following SARS-CoV-2 infection results in substantial increase of  
36 amounts of intravascular pro-coagulant extracellular vesicles (EV) expressing tissue factor  
37 (CD142) on their surface. CD142-EV turned out to be useful as diagnostic biomarker in  
38 COVID-19 patients. Here we aimed at studying the prognostic capacity of CD142-EV in  
39 SARS-CoV-2 infection.

40 Expression of CD142-EV was evaluated in 261 subjects admitted to hospital for pneumonia  
41 and with a positive molecular test for SARS-CoV-2. The study population consisted of a  
42 discovery cohort of selected patients (n=60) and an independent validation cohort including  
43 unselected consecutive enrolled patients (n=201). CD142-EV levels were correlated with  
44 post-hospitalization course of the disease and compared to the clinically available 4C  
45 Mortality Score as referral.

46 CD142-EV showed a reliable performance to predict patient prognosis in the discovery  
47 cohort (AUC=0.906) with an accuracy of 81.7%, that was confirmed in the validation cohort  
48 (AUC=0.736). Kaplan-Meier curves highlighted a high discrimination power in unselected  
49 subjects with CD142-EV being able to stratify the majority of patients according to their  
50 prognosis. We obtained a comparable accuracy, being not inferior in terms of prediction of  
51 patients' prognosis and risk of mortality, with 4C Mortality Score. The expression of surface  
52 vesicular CD142 and its reliability as prognostic marker was technically validated using  
53 different immunocapture strategies and assays.

54 The detection of CD142 on EV surface gains considerable interest as risk stratification tool  
55 to support clinical decision making in COVID-19.

56

57 **KEYWORDS**

58 CD142, tissue factor, SARS-CoV2, COVID-19, extracellular vesicles

59

60 **LIST OF ABBREVIATIONS**

61 Extracellular Vesicles, EVs; Immuno-Capture, IC; OroTracheal Intubation, OTI; Median  
62 Fluorescence Intensity, MFI; normalized MFI, nMFI; Severe Acute Respiratory Syndrome  
63 CoronaVirus 2, SARS-CoV-2; Tissue Factor, TF; Tissue Factor-positive EVs, EV-TF or  
64 CD142-EV; Ultra Centrifugation, UC; Western Blot, WB.

65 **1. INTRODUCTION**

66 The severe acute respiratory syndrome coronavirus 2 (SARS-CoV-2) has infected more  
67 than 455 million subjects as of 12 March 2022 (<https://coronavirus.jhu.edu>). The resulting  
68 disease (COVID-19) is associated with high hospitalization rates and an increased risk of  
69 respiratory failure, thus determining tremendous burden on the healthcare system of several  
70 countries and affecting the best possible care for patients.<sup>1,2</sup>A pragmatic risk score that uses  
71 analytic assay to estimate poor outcome from infection may assist medical staff in tailoring  
72 management strategies for patients and allocating limited healthcare resources.<sup>3</sup> Several  
73 prognostic models have been approached in the past two years to meet the urgent need of  
74 an efficient and early prognosis in patients with a confirmed diagnosis of COVID-19 for  
75 mortality risk, progression to severe disease and intensive care unit admission.<sup>3</sup> The most  
76 frequently used prognostic factors including age, image features, lymphocyte count and C-  
77 reactive protein, showed moderate performance in terms of clinical decision making.<sup>3, 4</sup> A  
78 clinically applicable prediction model with very good discrimination and performance  
79 characteristic has recently been validated in large cohort of patients.<sup>5</sup> The 4C Mortality Score  
80 including eight variables at hospital admission, outperformed other risk stratification tools  
81 and showed clinical decision making utility.<sup>5</sup>

82 Over the years, several studies have described the potential value of circulating extracellular  
83 vesicles (EVs) as prognostic biomarkers.<sup>6-10</sup> Molecular profiles of circulating EVs turned out  
84 to be useful as early prediction tool of COVID-19 severity.<sup>11</sup> Very recently, the total number  
85 of tissue factor-positive EVs (EV-TF) as well as their enzymatic activity were significantly  
86 associated with an increased severity risk in COVID-19 patients.<sup>12-14</sup>

87 In line with these studies we have lately showed that the expression of TF onto surface of  
88 EV isolated from COVID-19 patients serum was significantly higher than EVs isolated from  
89 healthy subjects as well as from those isolated from serum of subjects with pneumonia but  
90 different etiology from SARS-CoV-2.<sup>16</sup> Furthermore, the levels of expression of TF-bearing  
91 EV (CD142-EV) was significantly correlated with the capacity of EVs to generate factor Xa.<sup>16</sup>  
92 Contextually we produced very preliminary evidence showing that TF was significantly more  
93 expressed in severe COVID-19 patients undergoing orotracheal intubation (OTI) and/or  
94 death. However, we could not assess the performance of such EV marker as prognostic  
95 indicator due to the limited number of included patients. This paved the way for exploring  
96 the potential of this specific surface antigen as indicator of disease prognosis in a larger  
97 cohort of patients. The scientific endeavor of the present paper relies on the inclusion of 261  
98 laboratory-confirmed COVID-19 patients hospitalized for pneumonia, who underwent blood

99 sampling at time of molecular swab test and were longitudinally monitored to assess the  
100 clinical progression of disease. The expression of EV-associated TF was then  
101 retrospectively correlated with the course of the disease and its clinical performance was  
102 evaluated with the incidence of OTI and/or death as indicator of poor prognosis. The 4C  
103 Mortality Score was used as gold standard referral trying to put our experimental tool into  
104 scale with a widely validated in-use model.<sup>5</sup> We took advantage from reproducible flow  
105 cytometer assay that has been previously standardized and validated for the detection and  
106 characterization of EV surface signatures.<sup>17-20</sup>

107

## 108 **2. METHODS**

109 Supporting data for the present study are available within the article and the supplementary  
110 material. Because of their sensitive nature, additional information and single patient data  
111 are available from the corresponding author upon reasonable request.

112

### 113 **2.1 Patient recruitment**

114 The study was approved by the local ethical. Subjects gave informed consent according to  
115 the Declaration of Helsinki. The study population consists of 261 Caucasian white subjects  
116 hospitalized for pneumonia and SARS-CoV-2 infection at Internal Medicine Department and  
117 Cardiocentro Ticino Institute, Ente Ospedaliero Cantonale, Lugano, Switzerland. All patients  
118 were positive for SARS-CoV-2 as for molecular tests (polymerase chain reaction). Serum  
119 samples were collected at the time of nasopharyngeal swab sampling. The study population  
120 consisted in a discovery cohort (n=60) composed by selected patients admitted to hospital  
121 in March 2020, and in a validation cohort (n=201) composed by unselected consecutive  
122 patients admitted to hospital between April 2020 and May 2020. Patients were included in  
123 the study if they met the following criteria: infection by SARS-CoV-2, diagnosis of pneumonia  
124 and admission to hospital. Exclusion criteria were: (1) Age lower than 18 years; (2)  
125 Pregnancy; (3) Concomitant acute non-respiratory infection; (4) Cancer (active or recent  
126 history); (5) Inappropriateness to invasive emergency treatment (i.e., orotracheal intubation,  
127 advanced life support). Patients were classified in terms of outcome in good vs. poor  
128 prognosis, the latter was defined as need of orotracheal intubation, OTI, and/or death.

129

### 130 **2.2 Sample handling**

131 Peripheral venous blood samples were collected in serum separator tubes and maintained  
132 30 min at room temperature before centrifugation. After clot formation, blood underwent

133 serial low speed centrifugations at 4°C (1'600 x g for 10 min; 3'000 x g for 20 min; 10'000 x  
134 g for 15 min) to separate serum and to remove cellular debris and larger vesicles. Cleared  
135 serum was then aliquoted, stored at -80°C and never thawed prior to analysis.

136

## 137 **2.3 EV characterization**

138 **2.3.1 Bead-based EV surface profiling.** Serum samples underwent bead-based EV-  
139 capture and flow cytometric analysis by MACSPlex human Exosome Kit (Miltenyi) without  
140 further pre-isolation step, as previously described<sup>16, 21</sup>. EVs were isolated using capture-  
141 beads coated with antibodies coated with 37 different surface antigens and then analyzed  
142 after incubation with a detection reagent (labelled antibodies against CD9-CD63-CD81).  
143 Median fluorescence intensity (MFI; expressed as arbitrary unit, a.u.) was measured by  
144 MACSQuant Analyzer 10 flow cytometer (Miltenyi). Expression levels for each EV surface  
145 antigen were reported after subtraction for the respective fluorescence values of blank  
146 control and normalization for mean MFI for CD9/CD63/CD81 (normalized MFI, nMFI;  
147 expressed as percentage, %).<sup>17,18</sup> A reverse flow cytometric assay was also performed by  
148 isolating EVs by capture beads coated with antibodies against CD9-CD63-CD81 (EpCam;  
149 JSR Micro) and then incubated with fluorochrome-conjugated antibodies against CD142,  
150 and CD63 (as normalizator). MFI was measured CytoFLEX (Beckman Coulter).

151 **2.3.2 Western blot.** WB was performed on protein lysate after EV bead-based immuno-  
152 capture. Serum aliquots were incubated overnight with MACSPlex capture beads and saline  
153 solution. Unbounded fraction was discarded, and samples were lysed in RIPA buffer; total  
154 proteins were separated on SDS Page 4-12% gel (BioRad) and signals were detected by  
155 Odyssey CLx Detection System (LI-COR Biosciences). Blots for 3 representative samples  
156 were incubated with the following primary antibodies: rabbit polyclonal anti-ApoB48, mouse  
157 monoclonal anti-GRP94, rabbit monoclonal anti-Alix, rabbit monoclonal anti-CD142, rabbit  
158 monoclonal anti-TSG101, rabbit polyclonal anti-Syntenin-1, rabbit monoclonal anti-CD81 (all  
159 from Abcam), and rabbit monoclonal anti-Mitofillin (Invitrogen).

160 **2.3.3 Activity assay.** The activity assay for CD142 on EVs was performed with Human  
161 Tissue Factor Activity Assay (Abcam), according to manufacturer instructions. The protocol  
162 assesses amidolytic activity of TF/FVIIa complex to activate factor X (FX) to factor Xa.

163 **2.3.4 Co-localization assay (ExoView).** Co-localization was assessed by on-chip EV  
164 analysis using ExoView® R100 Analyzer, as previously described.<sup>22,23</sup> Functionalized chips  
165 were spotted with a solution of a mixture of anti-tetraspanin antibodies (CD9-CD63-CD81;  
166 Ancell). Serum samples incubated on chips for 2 hours at room temperature; chips were

167 than stained with a mixture of labelled antibodies against CD9-CD63-CD81 (Ancell), and for  
168 the CD142 co-localization assay, with antibody anti-TF (Invitrogen).

169

## 170 **2.4 Statistical analysis**

171 We expressed variables with a normal distribution as mean  $\pm$  standard deviation and their  
172 analysis was performed by T-student test. We expressed variables with a non-normal  
173 distribution as median [interquartile range] and their analysis was performed by Mann-  
174 Whitney test. Categorical variables were expressed as absolute number (percentage) and  
175 analyzed by Chi square test (or Fisher test, when appropriated). *P*-value of less than 0.05  
176 were considered significant. Logistic regression analysis was performed to assess the  
177 association of EV surface antigens with the outcome of patients. Hazard ratios (HRs) were  
178 evaluated together with their 95% confidence intervals. Receiver Characteristics Operating  
179 (ROC) curves were drawn to estimate the area under the curve (AUC) for EV surface  
180 antigens, to estimate their prediction performance (patient outcome). Statistics was  
181 performed by IBM SPSS Statistics 26 (IBM, New York, USA) and GraphPad PRISM 8.0 (La  
182 Jolla, California). For Estimation of study power see detailed method in supplementary file.

183

## 184 **3. RESULTS**

### 185 **3.1 Characteristics of the study cohorts**

186 We enrolled a total of 261 subjects with SARS-CoV-2 infection confirmed by PCR molecular  
187 test and admitted to hospital with a diagnosis of pneumonia (Table). Mean age was 68 years,  
188 65.5% were males, 62.1% displayed bilateral pneumonia, and 1.1% suffered from  
189 pulmonary embolism at hospitalization. Patients were stratified according to their outcome:  
190 36% needed to be treated with high flow O<sub>2</sub>, 13.8% underwent OTI, while the overall  
191 mortality was 19.2%. A poor prognosis, defined as needed of OTI or death, was reported in  
192 72 patients (27.6%); the median time from hospitalization to OTI/death was 7 days. As  
193 expected, the median duration of hospitalization was longer for patients with a poor  
194 prognosis compared to those with a good one (14 vs. 8 days).

195 Patients with a poor prognosis showed a higher incidence of bilateral pneumonia, a higher  
196 respiratory rate, and a lower peripheral O<sub>2</sub> saturation at admission. Moreover, they suffered  
197 from a higher number of comorbidities, and in particular chronic kidney disease, chronic  
198 heart failure, coronary artery disease, liver disease, chronic neurological conditions, and  
199 dementia. Concerning biochemical parameters, patients with a poor prognosis displayed  
200 higher values of lactic acid, C-reactive protein, D-dimer, aPTT, urea, and troponin I, and

201 lower levels of pO<sub>2</sub> at arterial blood gas analysis ( $p < 0.05$  for all comparisons; Table); no  
202 difference was found evaluating levels of haemoglobin, white blood cells and platelets count.  
203 The study population consisted in a first cohort of selected patients (discovery cohort;  $n = 60$ ),  
204 which was used to identify the detection threshold of CD142 expressed as nMFI (see  
205 methods) and corresponding to the expression level of such antigen onto surface of EV, that  
206 could be used as cut-off value to predict SARS-CoV-2 prognosis. Following the same criteria  
207 of inclusion as for the discovery cohort, a second prospective group composed by  
208 unselected consecutive patients was included as validation cohort ( $n = 201$ ). An overview of  
209 study design is depicted in Online Figure 1. Characteristics of discovery and validation  
210 cohorts are reported in Online Tables 1-3.

211

### 212 **3.2 EV profiling and selection of CD142-EV as biomarker to predict patient outcome**

213 The bead-based immunocapture flow cytometric assay used for EV profiling was first  
214 validated for its specificity to bind EVs by western blot for specific markers and potential  
215 contaminants and flow cytometry for tetraspanins expression on EV surface (Supplementary  
216 Results; Online Figure 2). We then evaluated the expression of 37 EV surface antigens in  
217 all recruited patients (discovery and validation cohort;  $n = 261$ ) and compared their  
218 fluorescence levels in patients with SARS-CoV2 infection after stratification for prognosis  
219 (Online Tables 4-5) and mortality (Online Tables 6-7). The EV surface signature in patients  
220 stratified according to their prognosis is shown in Online Figures 3 and 4.

221 In the discovery cohort ( $n = 60$ ), among the differentially expressed surface epitopes in  
222 patients with good vs. poor prognosis (CD49e, CD69, CD142, and CD45; see  
223 Supplementary Results, Figure 1A and Online Table 4), CD142-EV displayed the strongest  
224 association with prognosis with a hazard ratio (HR) of 1.074 (95% CI 1.032-1.119) at  
225 regression models, thus meaning that for each single unit of increase in nMFI for this EV  
226 marker, the risk of a poor prognosis increased of 7.4% (Figure 1B and Online Table 8). At  
227 ROC curve analysis, CD142-EV had an AUC of 0.906 (95% CI 0.833-0.979) with an  
228 accuracy of 81.7% (Figure 1C and Online Table 9), using a cut-off value of 33.5 (nMFI, %).  
229 After stratification for mortality, CD4, CD142 and CD45 were highly expressed in deceased  
230 patients (see Supplementary Results, Figure 1D and Online Table 6). CD142-EV was again  
231 di best predictor, with an HR of 1.039 (95% CI 1.018-1.057), thus meaning an increase of  
232 3.9% in mortality rate, for each unit of increase in nMFI of the marker (Figure 1E and Online  
233 Table 8). The analysis of ROC curve showed an AUC of 0.842 (95% CI 0.727-0.957) with



234 an accuracy of 85% to predict mortality (Figure 1F and Online Table 10), using a cut-off  
235 value of 52.8 (nMFI, %).

236

### 237 **3.3 CD142-EV discriminates SARS-CoV2 patients according to prognosis**

238 In the discovery cohort a cut-off greater than 33.5 (nMFI, %) for CD142-EV correctly  
239 identified 18 out of 24 patients with a poor prognosis (sensitivity 75%), while those with an  
240 nMFI equal or lower to 33.5 displayed a good prognosis in 31 out of 36 cases (specificity  
241 86.1%; Figure 2A and Online Tables 11-12). The potential of CD142-EV as discriminant for  
242 subjects belonging to the discovery cohort was further assessed by Kaplan-Meier curves  
243 showing a log-rank of 4.75 (95% CI 2.09-10.81; Figure 2B). By applying the same cut-off in  
244 the validation cohort (unselected subjects), we were still able to correctly classify 131 out of  
245 153 patients with a good prognosis (specificity 85.6%) and a high negative predictive value  
246 (86.2%). The overall accuracy was 78.6%, with a negligible overfitting bias (3.1%) when  
247 compared with accuracy in the discovery cohort (Figure 2A). Kaplan-Meier curves further  
248 confirmed a high discrimination power, with CD142-EV able to correctly stratify 158 out of  
249 201 patients according to prognosis (good vs. poor prognosis; log-rank = 2.22 - 95% CI  
250 1.23-3.99; Figure 2C).

251

### 252 **3.4 CD142-EV discriminates SARS-CoV2 patients according to mortality**

253 Considering the outcome of survival as for the ROC analysis, the nMFI value of 52.8% was  
254 selected as critical cut-off for CD142-EV (Figure 3A;). Such value allowed the classification  
255 of 51 out of 60 patients in the discovery cohort, resulting in an accuracy of 85%, with a  
256 sensitivity and specificity of 75.0% and 87.5%, respectively (Online Tables 11-12). Kaplan-  
257 Meier curves showed that CD142-EV was able to stratify patient according to their mortality  
258 in discovery cohort with a log-rank = 11.30 (95% CI 2.82-45.34 Figure 3B). At validation, we  
259 correctly predicted the survival of 152 out of 163 patients (specificity 94.3%), once again  
260 with a high negative predictive value (85.9%) and an overall accuracy of 82.1% with an  
261 overfitting bias of 2.9% (Figure 3A). The discrimination power according to mortality (Kaplan-  
262 Meier curves) was consistent with 165 out of 201 patients correctly predicted (survival; log-  
263 rank = 3.37 - 95% CI 1.27-8.93; Figure 3C).

264

### 265 **3.5 CD142-EV predict prognosis and mortality in SARS-CoV2**

266 Having assessed the performance of CD142-EV as prognostic tool, we applied such  
267 unconventional biomarker to the entire population of included patients (discovery plus

268 validation cohort), to assess patient distribution according to outcome and expression levels  
269 of CD142-EV. The likelihood of a poor prognosis, as well as mortality, gradually increased  
270 at the increase of nMFI for CD142-EV (Figures 2D-3D). Among patients with lowest score  
271 (CD142-EV  $\leq 10$ ) 107 out of 117 displayed good prognosis (91.5%), and 108 out of 120  
272 (90.0%) were alive at follow-up. Thus, translating in a very high specificity and negative  
273 predictive value (Online Table 13). Conversely, among patients with the highest score  
274 (CD142-EV  $>70$ ), 22 out of 23 (95.7%) displayed a poor prognosis and 15 out of 25 (60%)  
275 deceased at follow-up, with a very high sensitivity and positive predictive value (Online Table  
276 13). For each patient, we calculated the 4C (Coronavirus Clinical Characterization  
277 Consortium) Mortality score as described in Knight SR et al.<sup>5</sup> 4C Mortality score was then  
278 used as referral to estimate the potential application of our experimental model based on  
279 CD142-EV in predicting patient prognosis and mortality (Online Figure 5; Online Table 11).  
280 Considering all patients CD142-EV showed a higher accuracy compared to 4C score in  
281 predicting patient prognosis (AUC 0.792 vs. 0.705 –  $p=0.044$ ; accuracy 79.3% vs. 67.8%;  
282 Figure 2E), whereas the overall accuracy was comparable when predicting mortality (AUC  
283 0.714 vs. 0.786;  $p=0.131$ ; accuracy 82.3% vs. 73.9%; Figure 3E). Diagnostic performance  
284 and confusion matrix of CD142-EV and 4C Mortality score to predict either patient prognosis  
285 or mortality, are summarized in Online Table 12.

286

### 287 **3.6 CD142-EV experimental validation as biomarker in SARS-CoV2**

288 We have previously shown that TF expressed on the surface of EV possess enzymatic  
289 activity which directly correlate with its level of expression.<sup>16</sup> Here, we assessed whether  
290 such activity has also potential as prognostic marker, as further confirmation of CD142-EV  
291 as predictor of patient outcome in SARS-CoV2. EVs isolated by ultracentrifugation (UC) and  
292 by immuno-capture beads (IC) from serum of 20 randomly selected patients from the  
293 validation cohort (10 with a good prognosis and 10 with a poor prognosis) were quantitatively  
294 measured for CD142 enzymatic activity. Both, EVs enriched by classical UC or using IC  
295 showed an augmented CD142 activity when isolated from serum of patients with poor vs.  
296 good prognosis ( $p<0.05$ ; Figure 4A-B). Notably, CD142-EV level of expression measured  
297 at flow cytometry directly correlated to CD142 activity measured by ELISA ( $R=0.720$ ;  
298  $p<0.001$ ; Figure 4C).

299 To overcome possible methodological- or instrumental-related biases, the expression of  
300 surface vesicular CD142 was also measured by using a reverse immunocapture strategy.  
301 Indeed, EV were captured by using beads coated with antibodies direct against tetraspanins

302 and immuno-stained for CD142. We confirmed that the level of expression of CD142 was  
303 significantly higher in EV from patients with poor vs. good prognosis regardless the protocol  
304 of EV binding ( $p < 0.01$ ; Figure 4D).

305 Finally, we further assessed the co-localization of tetraspanins with CD142 by ExoView®  
306 Analyzer which allowed the immunocapture of EV onto silico chip and the simultaneously  
307 detection of surface antigens CD9, CD63, CD81 and CD142, (Figure 4E). The assay  
308 confirmed that EV specific tetraspanins are mainly co-expressed with tissue factor. By  
309 quantifying the degree of expression of each marker, we could further confirm that the  
310 number of total tetraspanin positive EV as well as the number of CD142-bearing EV, were  
311 both increased in patients with more severe disease (FC 1.4 -  $p = 0.005$ , and FC 3.5 -  
312  $p = 0.002$ , respectively).

313

#### 314 **4. DISCUSSION**

315 We have addressed the potential value of CD142-EV as prognostic biomarker in a cohort of  
316 patients admitted to hospital for pneumonia and SARS-CoV-2 infection. Both the discovery  
317 and the validation cohorts were tailored on reliable estimation of minimum number of  
318 subjects to be included on the base of our previous pilot study.<sup>16</sup> By using this prospective  
319 cohort of unselected patients consecutively recruited, we obtained an overall accuracy of  
320 78.6% and 82.1% in predicting patient prognosis and mortality, respectively. Noteworthy,  
321 CD142-EV reached a reliable grade of “generalizability” as prognostic marker since the  
322 overfitting bias was negligible when comparing accuracy in the discovery and validation  
323 cohorts (ranging between 2.9 and 3.1%).

324 CD142-EV performed well against the clinically applied 4C Mortality Score, which is  
325 currently one of the most robustly validated COVID-19 prognostic model.<sup>5</sup> When considering  
326 all patients, we obtained an overall comparable accuracy, being not inferior in terms of  
327 prediction of patients’ prognosis (overall accuracy 79.3% CD142-EV vs. 67.8% 4C Mortality  
328 Score) and risk of mortality (overall accuracy 82.3% CD142-EV vs. 73.9% 4C Mortality  
329 Score). CD142-EV displayed a very high specificity and negative predictive value (ranging  
330 between 83.4 and 93.3%). However, as compared to 4C Mortality score it shows lower  
331 sensitivity and positive predictive value (ranging between 34.2-78.2%), thus making CD142-  
332 EV mainly suitable to rule out severe cases. CD142-EV also performed well in stratifying  
333 patients according to their risk of a poor prognosis. The likelihood of a poor outcome (OTI  
334 and/or death) gradually increases with CD142-EV expression and therefore it was suitable  
335 for the quantification of a discrete risk. For instance, patients with a CD142-EV nMFI ranging

336 between 20 and 30 display a likelihood of 25% and 13% in terms of poor prognosis and  
337 mortality respectively. On the other hand, patients with CD142-EV ranging between 60 and  
338 70 will have a poor prognosis in 75% of cases, with a mortality of 42.9%.

339 Although patients for validation have been enrolled by avoiding selection bias, the cohort  
340 still suffer of the limited number of enrolled subjects. Such small cohort of validation also  
341 represents the main limit for more in-depth comparison with 4C Mortality Score that included  
342 more than 22000 subjects in validation. A further limitation includes the fact that the study  
343 was temporally and geographically narrowed. Infection rates and patients' characteristics  
344 might change by time and geography during a pandemic. Here we could not show  
345 robustness of the CD142-EV over time and geography.

346 We do not add substantial advancing in the debate concerning whether it is better to  
347 measure levels of TF activity or TF protein as marker of thrombotic risk,<sup>24, 25</sup> however we  
348 clearly show that the TF protein level on the surface of EV consistently predict the severity  
349 of COVID-19 disease. We have also shown that CD142-bearing EVs have an augmented  
350 enzymatic activity when isolated from serum of patients with severe disease and a poor  
351 prognosis, regardless the method of isolation. Finally, we showed that the level of  
352 expression of TF strongly correlates with its activity in COVID-19 patients and it is hampered  
353 when using specific antibody that causes steric hindrance with the enzymatic site of the  
354 TF.<sup>16</sup> It is plausible, and some recently published data come in help supporting this  
355 hypothesis, that both parameters are associated with severity of disease in COVID-19  
356 patients.<sup>12, 13, 15</sup> The discrepancy between protein expression and activity, due to the  
357 presence of undefined portion of intravascular TF present as inactive or encrypted state,<sup>26</sup>  
358 is negligible when referring to EVs. The cytokines storm<sup>27</sup> as well as the hyper-activation of  
359 platelets<sup>12</sup> occurring in these patients may dramatically contribute to increase the release of  
360 EV with pro-coagulant activity, thus expressing TF in a decrypted state.<sup>28</sup> As respect to  
361 Guervilly et al. we found significant increase in the total amount of circulating EV in patients  
362 with poor versus good prognosis. The apparent discrepancy might be explained by the fact  
363 that we only addressed concentration (expressed as nMFI) of CD9; CD81 and CD63 positive  
364 EV, while a direct FC assay as in Guervilly et al. can account for enumeration of large  
365 vesicles that can be negative for tetraspanins while still expressing TF.<sup>15</sup> A second possible  
366 explanation reside in the starting material as EV source: we used serum in stand of plasma.  
367 We are aware that this aspect may represent a weakness of the study, however we have  
368 previously shown that the profiling of EV from serum has good potential as biomarker,  
369 showing consistent diagnostic and prognostic performances, in line with gold-standard

370 biomarkers.<sup>29</sup> Both plasma and serum have been used in previous studies; while biobanking  
371 of plasma may be preferable for studies involving isolation of EV, RNA or functional in vitro  
372 / in vivo assays, serum also has appropriate uses.<sup>30</sup> Above all, the prognostic performance  
373 of serum CD142-EV is in line with others regardless EV's sources.<sup>12,14,15</sup> The methodological  
374 assessment of the most appropriate biological fluid is beyond the scope of the present study.

375

## 376 **5. CONCLUSIONS**

377 The aim of the present study was to give clinical relevance to a biomarker that can be useful  
378 to assess the risk of negative outcome and to prompt the adoption of strategies to treat the  
379 disease. Indeed, the detection of CD142 on the surface of EV is a cost-effective and rapid  
380 test that can be available at time of admission by using conventional flow cytometer. The  
381 method used is well standardized from our group<sup>21, 31</sup> as well as from other independent  
382 groups<sup>17, 18</sup> from sample preparation to data analysis, ensuring that results can be  
383 reproducible and shared among different laboratories. We believe that such analysis gains  
384 considerable interest as risk stratification tool to support frontline clinical decision making.

385

386

387 **Acknowledgments.** Visual abstract was produced using Servier Medical Art  
388 (<https://smart.servier.com/>).

389 **Author Contributions.** J.B. data generation and interpretation, statistical analysis,  
390 manuscript writing. E.C., L.G.G., E.R., T.F.S., and E.F., patient data collection. E.P., and  
391 G.Ma. sample collection. A.B. statistical analysis. C.B., S.B., E.L., V.B., R.F., A.G., M.C.,  
392 G.V., and G.Me. data generation and interpretation, critical revision. S.M., and L.B. study  
393 design, data interpretation, manuscript writing. All authors read and approved the final  
394 version of the manuscript.

395 **Conflict of interest.** Authors have nothing to disclose.

396 **Funding.** This study was supported by research funding from Fidnam Foundation (Lugano,  
397 Switzerland).

398 **REFERENCES**

- 399 1. Arabi YM, Murthy S, Webb S. Covid-19: A novel coronavirus and a novel challenge for  
400 critical care. *Intensive Care Med.* 2020;46:833-836
- 401 2. Yang X, Yu Y, Xu J, Shu H, Xia J, Liu H, Wu Y, Zhang L, Yu Z, Fang M, Yu T, Wang Y,  
402 Pan S, Zou X, Yuan S, Shang Y. Clinical course and outcomes of critically ill patients  
403 with sars-cov-2 pneumonia in wuhan, china: A single-centered, retrospective,  
404 observational study. *Lancet Respir Med.* 2020;8:475-481
- 405 3. Wynants L, Van Calster B, Collins GS, Riley RD, Heinze G, Schuit E, Bonten MMJ,  
406 Dahly DL, Damen JAA, Debray TPA, de Jong VMT, De Vos M, Dhiman P, Haller MC,  
407 Harhay MO, Henckaerts L, Heus P, Kammer M, Kreuzberger N, Lohmann A, Luijken K,  
408 Ma J, Martin GP, McLernon DJ, Andaur Navarro CL, Reitsma JB, Sergeant JC, Shi C,  
409 Skoetz N, Smits LJM, Snell KIE, Sperrin M, Spijker R, Steyerberg EW, Takada T,  
410 Tzoulaki I, van Kuijk SMJ, van Bussel B, van der Horst ICC, van Royen FS, Verbakel  
411 JY, Wallisch C, Wilkinson J, Wolff R, Hooft L, Moons KGM, van Smeden M. Prediction  
412 models for diagnosis and prognosis of covid-19: Systematic review and critical  
413 appraisal. *BMJ.* 2020;369:m1328
- 414 4. Gupta RK, Marks M, Samuels THA, Luintel A, Rampling T, Chowdhury H, Quartagno  
415 M, Nair A, Lipman M, Abubakar I, van Smeden M, Wong WK, Williams B, Noursadeghi  
416 M, Group UC-R. Systematic evaluation and external validation of 22 prognostic models  
417 among hospitalised adults with covid-19: An observational cohort study. *Eur Respir J.*  
418 2020;56
- 419 5. Knight SR, Ho A, Pius R, Buchan I, Carson G, Drake TM, Dunning J, Fairfield CJ,  
420 Gamble C, Green CA, Gupta R, Halpin S, Hardwick HE, Holden KA, Horby PW, Jackson  
421 C, McLean KA, Merson L, Nguyen-Van-Tam JS, Norman L, Noursadeghi M, Olliaro PL,  
422 Pritchard MG, Russell CD, Shaw CA, Sheikh A, Solomon T, Sudlow C, Swann OV,  
423 Turtle LC, Openshaw PJ, Baillie JK, Semple MG, Docherty AB, Harrison EM,  
424 investigators IC. Risk stratification of patients admitted to hospital with covid-19 using  
425 the isaric who clinical characterisation protocol: Development and validation of the 4c  
426 mortality score. *BMJ.* 2020;370:m3339
- 427 6. Zacharia E, Zacharias K, Papamikroulis GA, Bertsias D, Miliou A, Pallantza Z,  
428 Papageorgiou N, Tousoulis D. Cell-derived microparticles and acute coronary  
429 syndromes: Is there a predictive role for microparticles? *Curr Med Chem.* 2020;27:4440-  
430 4468

- 431 7. Chiva-Blanch G, Crespo J, Suades R, Arderiu G, Padro T, Vilahur G, Cubedo J, Corella  
432 D, Salas-Salvado J, Aros F, Martinez-Gonzalez MA, Ros E, Fito M, Estruch R, Badimon  
433 L. Cd142+/cd61+, cd146+ and cd45+ microparticles predict cardiovascular events in  
434 high risk patients following a mediterranean diet supplemented with nuts. *Thrombosis  
435 and haemostasis*. 2016;116:103-114
- 436 8. Huo S, Krankel N, Nave AH, Sperber PS, Rohmann JL, Piper SK, Heuschmann PU,  
437 Landmesser U, Endres M, Siegerink B, Liman TG. Endothelial and leukocyte-derived  
438 microvesicles and cardiovascular risk after stroke: Proscis-b. *Neurology*. 2021;96:e937-  
439 e946
- 440 9. Camera M, Brambilla M, Canzano P, Cavallotti L, Parolari A, Tedesco CC, Zara C,  
441 Rossetti L, Tremoli E. Association of microvesicles with graft patency in patients  
442 undergoing cabg surgery. *J Am Coll Cardiol*. 2020;75:2819-2832
- 443 10. Vacchi E, Burrello J, Di Silvestre D, Burrello A, Bolis S, Mauri P, Vassalli G, Cereda CW,  
444 Farina C, Barile L, Kaelin-Lang A, Melli G. Immune profiling of plasma-derived  
445 extracellular vesicles identifies parkinson disease. *Neurol Neuroimmunol  
446 Neuroinflamm*. 2020;7
- 447 11. Fujita Y, Hoshina T, Matsuzaki J, Yoshioka Y, Kadota T, Hosaka Y, Fujimoto S,  
448 Kawamoto H, Watanabe N, Sawaki K, Sakamoto Y, Miyajima M, Lee K, Nakaharai K,  
449 Horino T, Nakagawa R, Araya J, Miyato M, Yoshida M, Kuwano K, Ochiya T. Early  
450 prediction of covid-19 severity using extracellular vesicle copb2. *J Extracell Vesicles*.  
451 2021;10:e12092
- 452 12. Canzano P, Brambilla M, Porro B, Cosentino N, Tortorici E, Vicini S, Poggio P, Cascella  
453 A, Pengo MF, Veglia F, Fiorelli S, Bonomi A, Cavalca V, Trabattoni D, Andreini D,  
454 Omodeo Sale E, Parati G, Tremoli E, Camera M. Platelet and endothelial activation as  
455 potential mechanisms behind the thrombotic complications of covid-19 patients. *JACC  
456 Basic Transl Sci*. 2021
- 457 13. Rosell A, Havervall S, von Meijenfildt F, Hisada Y, Aguilera K, Grover SP, Lisman T,  
458 Mackman N, Thalín C. Patients with covid-19 have elevated levels of circulating  
459 extracellular vesicle tissue factor activity that is associated with severity and mortality-  
460 brief report. *Arterioscler Thromb Vasc Biol*. 2021;41:878-882
- 461 14. Krishnamachary B, Cook C, Kumar A, Spikes L, Chalise P, Dhillon NK. Extracellular  
462 vesicle-mediated endothelial apoptosis and ev-associated proteins correlate with covid-  
463 19 disease severity. *J Extracell Vesicles*. 2021;10:e12117

- 464 15. Guervilly C, Bonifay A, Burtey S, Sabatier F, Cauchois R, Abdili E, Arnaud L, Lano G,  
465 Pietri L, Robert T, Velier M, Papazian L, Albanese J, Kaplanski G, Dignat-George F,  
466 Lacroix R. Dissemination of extreme levels of extracellular vesicles: Tissue factor  
467 activity in patients with severe covid-19. *Blood Adv.* 2021;5:628-634
- 468 16. Balbi C, Burrello J, Bolis S, Lazzarini E, Biemmi V, Pianezzi E, Burrello A, Caporali E,  
469 Grazioli LG, Martinetti G, Fusi-Schmidhauser T, Vassalli G, Melli G, Barile L. Circulating  
470 extracellular vesicles are endowed with enhanced procoagulant activity in sars-cov-2  
471 infection. *EBioMedicine.* 2021;67:103369
- 472 17. Koliha N, Wiencek Y, Heider U, Jungst C, Kladt N, Krauthauser S, Johnston IC, Bosio  
473 A, Schauss A, Wild S. A novel multiplex bead-based platform highlights the diversity of  
474 extracellular vesicles. *J Extracell Vesicles.* 2016;5:29975
- 475 18. Wiklander OPB, Bostancioglu RB, Welsh JA, Zickler AM, Murke F, Corso G, Felldin U,  
476 Hagey DW, Evertsson B, Liang XM, Gustafsson MO, Mohammad DK, Wiek C,  
477 Hanenberg H, Bremer M, Gupta D, Bjornstedt M, Giebel B, Nordin JZ, Jones JC, El  
478 Andaloussi S, Gorgens A. Systematic methodological evaluation of a multiplex bead-  
479 based flow cytometry assay for detection of extracellular vesicle surface signatures.  
480 *Front Immunol.* 2018;9:1326
- 481 19. Vacchi E, Burrello J, Burrello A, Bolis S, Monticone S, Barile L, Kaelin-Lang A, Melli G.  
482 Profiling inflammatory extracellular vesicles in plasma and cerebrospinal fluid: An  
483 optimized diagnostic model for parkinson's disease. *Biomedicines.* 2021;9
- 484 20. Castellani C, Burrello J, Fedrigo M, Burrello A, Bolis S, Di Silvestre D, Tona F, Bottio T,  
485 Biemmi V, Toscano G, Gerosa G, Thiene G, Basso C, Longnus SL, Vassalli G, Angelini  
486 A, Barile L. Circulating extracellular vesicles as non-invasive biomarker of rejection in  
487 heart transplant. *J Heart Lung Transplant.* 2020
- 488 21. Burrello J, Bianco G, Burrello A, Manno C, Maulucci F, Pileggi M, Nannoni S, Michel P,  
489 Bolis S, Melli G, Vassalli G, Albers GW, Cianfoni A, Barile L, Cereda CW. Extracellular  
490 vesicle surface markers as a diagnostic tool in transient ischemic attacks. *Stroke.*  
491 2021:STROKEAHA120033170
- 492 22. Gori A, Romanato A, Greta B, Strada A, Gagni P, Frigerio R, Brambilla D, Vago R,  
493 Galbiati S, Picciolini S, Bedoni M, Daaboul GG, Chiari M, Cretich M. Membrane-binding  
494 peptides for extracellular vesicles on-chip analysis. *J Extracell Vesicles.*  
495 2020;9:1751428



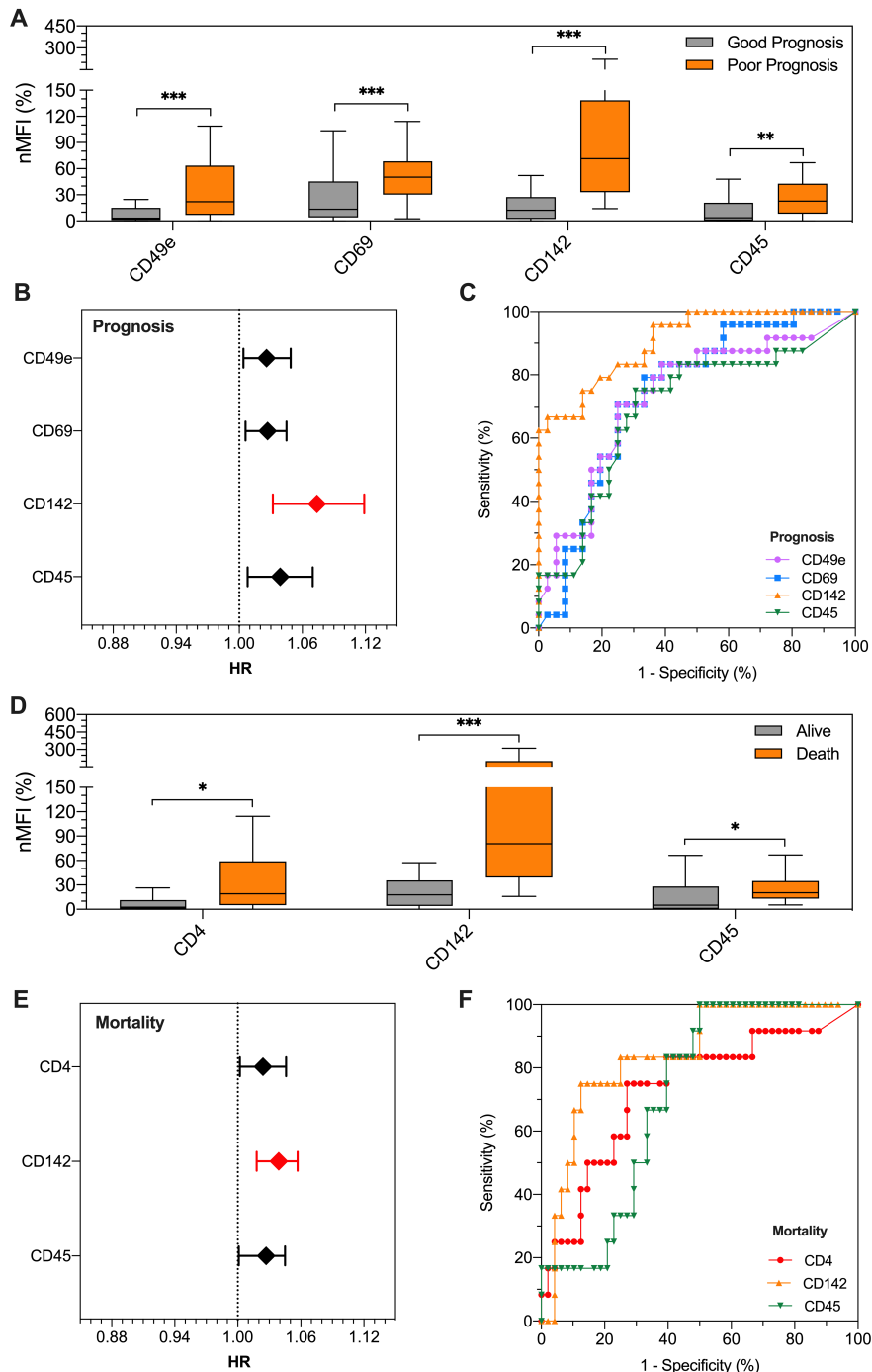
- 496 23. Daaboul GG, Gagni P, Benussi L, Bettotti P, Ciani M, Cretich M, Freedman DS, Ghidoni  
497 R, Ozkumur AY, Piotto C, Prosperi D, Santini B, Unlu MS, Chiari M. Digital detection of  
498 exosomes by interferometric imaging. *Sci Rep.* 2016;6:37246
- 499 24. Mackman N, Hisada Y, Grover SP, Rosell A, Havervall S, von Meijenfeldt F, Aguilera K,  
500 Lisman T, Thalín C. Response by mackman et al to letter regarding article, "patients  
501 with covid-19 have elevated levels of circulating extracellular vesicle tissue factor activity  
502 that is associated with severity and mortality-brief report". *Arterioscler Thromb Vasc Biol.*  
503 2021;41:e381-e382
- 504 25. Brambilla M, Canzano P, Becchetti A, Tremoli E, Camera M. Letter by brambilla et al  
505 regarding article, "patients with covid-19 have elevated levels of circulating extracellular  
506 vesicle tissue factor activity that is associated with severity and mortality-brief report".  
507 *Arterioscler Thromb Vasc Biol.* 2021;41:e379-e380
- 508 26. Rao LV, Kothari H, Pendurthi UR. Tissue factor encryption and decryption: Facts and  
509 controversies. *Thromb Res.* 2012;129 Suppl 2:S13-17
- 510 27. Yang L, Xie X, Tu Z, Fu J, Xu D, Zhou Y. The signal pathways and treatment of cytokine  
511 storm in covid-19. *Signal Transduct Target Ther.* 2021;6:255
- 512 28. Wang J, Pendurthi UR, Yi G, Rao LVM. Sars-cov-2 infection induces the activation of  
513 tissue factor-mediated coagulation by activation of acid sphingomyelinase. *Blood.* 2021
- 514 29. Burrello J, Bolis S, Balbi C, Burrello A, Provasi E, Caporali E, Gauthier LG, Peirone A,  
515 D'Ascenzo F, Monticone S, Barile L, Vassalli G. An extracellular vesicle epitope profile  
516 is associated with acute myocardial infarction. *J Cell Mol Med.* 2020
- 517 30. Witwer KW, Buzas EI, Bemis LT, Bora A, Lasser C, Lotvall J, Nolte-'t Hoen EN, Piper  
518 MG, Sivaraman S, Skog J, Thery C, Wauben MH, Hochberg F. Standardization of  
519 sample collection, isolation and analysis methods in extracellular vesicle research. *J*  
520 *Extracell Vesicles.* 2013;2
- 521 31. Burrello J, Tetti M, Forestiero V, Biemmi V, Bolis S, Pomatto MAC, Amongero M, Di  
522 Silvestre D, Mauri P, Vassalli G, Camussi G, Williams TA, Mulatero P, Barile L,  
523 Monticone S. Characterization of circulating extracellular vesicle surface antigens in  
524 patients with primary aldosteronism. *Hypertension.*  
525 2021:HYPERTENSIONAHA12117136
- 526 32. Charlson ME, Pompei P, Ales KL, MacKenzie CR. A new method of classifying  
527 prognostic comorbidity in longitudinal studies: Development and validation. *J Chronic*  
528 *Dis.* 1987;40:373-383

529 **Table 1. Patient characteristics**

Variable	All Patients [n=261]	Good Prognosis [n=189]	Poor Prognosis [n=72]	P-value
Age (years)	68 ± 13.4	68 ± 13.6	71 ± 12.8	0.100
Sex (Male; %)	171 (65.5)	119 (63.0)	52 (72.2)	0.160
BMI (Kg/sqm)	27.4 ± 5.67	27.0 ± 5.60	28.2 ± 5.78	0.204
Bilateral Pneumonia (%)	162 (62.1)	104 (55.0)	58 (80.6)	<b>&lt;0.001</b>
Pulmonary Embolism (%)	3 (1.1)	2 (1.1)	1 (1.4)	1.000
Respiratory rate (a.p.m.)	22 ± 5.0	20 ± 4.0	25 ± 5.6	<b>&lt;0.001</b>
Peripheral O <sub>2</sub> saturation (%)	92 ± 4.1	93 ± 3.5	90 ± 4.9	<b>&lt;0.001</b>
GCS (<15; n)	28 (10.7)	16 (8.5)	12 (16.7)	0.056
<i>Anamnesis</i>				
CKD (%)	44 (16.9)	16 (8.5)	28 (38.9)	<b>&lt;0.001</b>
Hypertension (%)	144 (55.2)	101 (53.4)	43 (59.7)	0.362
Chronic Pulmonary Disease (%)	46 (17.6)	30 (15.9)	16 (22.2)	0.229
Diabetes (%)	66 (25.3)	45 (23.8)	21 (29.2)	0.373
Smoking habit (%)	36 (13.8)	20 (10.6)	16 (22.2)	<b>0.015</b>
CHF (%)	20 (7.7)	10 (5.3)	10 (13.9)	<b>0.020</b>
CAD (%)	47 (18.0)	25 (13.2)	22 (30.6)	<b>0.001</b>
Liver Disease (%)	51 (19.5)	29 (15.3)	22 (30.6)	<b>0.006</b>
Chronic Neurological Disease (%)	58 (22.2)	36 (19.0)	22 (30.6)	<b>0.046</b>
Dementia (%)	39 (14.9)	22 (11.6)	17 (23.6)	<b>0.015</b>
Autoimmune Disease (%)	0 (0.0)	0 (0.0)	0 (0.0)	1.000
HIV/AIDS (%)	0 (0.0)	0 (0.0)	0 (0.0)	1.000
Cancer (%)	0 (0.0)	0 (0.0)	0 (0.0)	1.000
Obesity (%)	52 (19.9)	34 (18.0)	18 (25.0)	0.205
Number of Comorbidities (n)	1 [0; 2]	1 [0; 2]	2 [1; 4]	<b>&lt;0.001</b>
<i>Arterial blood gas assay</i>				
pCO <sub>2</sub> (KPa)	4.5 [4.1; 5.0]	4.5 [4.1; 4.9]	4.7 [4.0; 5.2]	0.171
pO <sub>2</sub> (KPa)	9.1 [8.1; 10.5]	9.3 [8.5; 10.8]	8.6 [7.7; 10.1]	<b>0.003</b>
Bicarbonate (mmol/L)	23.6 ± 3.10	23.8 ± 2.74	23.0 ± 3.85	0.163
Lactic acid (mmol/L)	1.3 ± 0.80	1.2 ± 0.69	1.5 ± 1.02	<b>0.049</b>
<i>Biochemical parameters</i>				
Haemoglobin (g/L)	139 ± 18.6	141 ± 17.4	135 ± 21.1	0.052
PLTS (*10E9/L)	190 ± 73.3	187 ± 71.4	199 ± 77.7	0.238
WBC (*10E9/L)	6.6 ± 3.30	6.4 ± 3.08	6.9 ± 3.80	0.242
Neutrophils (*10E9/L)	5.3 ± 4.22	5.3 ± 4.74	5.5 ± 3.61	0.806
Lymphocytes (*10E9/L)	1.0 ± 0.92	1.1 ± 0.84	0.9 ± 0.81	0.533
Monocytes (*10E9/L)	0.4 ± 0.23	0.4 ± 0.19	0.4 ± 0.30	0.868
Eosinophils (*10E9/L)	0.06 ± 0.043	0.06 ± 0.034	0.07 ± 0.029	0.780
Basophils (*10E9/L)	0.06 ± 0.051	0.05 ± 0.032	0.06 ± 0.028	0.905
C-reactive protein (mg/L)	47 [21; 98]	40 [18; 86]	69 [35; 137]	<b>0.003</b>
D-dimer (mg/L)	0.76 [0.50; 1.41]	0.67 [0.48; 1.15]	1.08 [0.66; 2.35]	<b>&lt;0.001</b>
PT-INR (a.u.)	1.2 ± 0.62	1.2 ± 0.53	1.4 ± 0.81	0.097
aPTT (sec)	32 ± 7.1	31 ± 6.1	34 ± 8.8	<b>0.031</b>
LDH (U/L)	467 [381; 633]	462 [375; 601]	484 [392; 776]	0.079
Urea (mmol/L)	7.2 ± 5.06	6.4 ± 3.50	9.4 ± 7.38	<b>0.001</b>
Troponin I (ng/L)	14 [8; 29]	12 [6; 19]	25 [13; 66]	<b>&lt;0.001</b>
<i>Outcome</i>				
4C Mortality Score (n)	9 ± 4.0	8 ± 3.7	11 ± 3.8	<b>&lt;0.001</b>
Hospitalization (days)	9 [2; 16]	8 [2; 14]	14 [7; 26]	<b>&lt;0.001</b>
Time to OTI / Death (days)	N.A.	N.A.	7 [4; 12]	N.A.
Low-flow O <sub>2</sub> Treatment (%)	222 (85.1)	158 (83.6)	64 (88.9)	0.284
High-flow O <sub>2</sub> Treatment (%)	94 (36.0)	41 (21.7)	53 (73.6)	<b>&lt;0.001</b>
Orotracheal Intubation (%)	36 (13.8)	N.A.	36 (50.0)	N.A.
Death (%)	50 (19.2)	N.A.	50 (69.4)	N.A.

530 **Legend to Table 1. Patient characteristics**

531 Clinical and biochemical characteristics of patients admitted to hospital for SARS-CoV2  
532 infection and pneumonia (n=261) stratified according to prognosis; a poor prognosis is  
533 defined as need of orotracheal intubation (OTI) or death. GCS, Glasgow Coma Scale; CKD,  
534 Chronic Kidney Disease (defined as eGFR < 60 mL/min); CHF, Chronic Heart Failure  
535 (defined as ejection fraction < 35%), CAD, Coronary Artery Disease; Liver disease, defined  
536 as chronic hepatitis or cirrhosis with or without portal hypertension; Chronic neurological  
537 disease, defined as presence of Parkinson disease, Alzheimer disease, history of major  
538 cerebrovascular accident; HIV/AIDS, infection by Human Immunodeficiency Virus, Acquired  
539 Immunodeficiency Syndrome; WBC, White Blood Cells; PT-INR, Thrombin Time -  
540 International Normalized Ratio; aPTT, activated Partial Thromboplastin Time; LDH, Lactate  
541 Dehydrogenase; N.A., Not Applicable. 4C Mortality Score was calculated as detailed in  
542 Knight SR et al 2020.<sup>5</sup> Comorbidities were defined using the Charlson comorbidities index.<sup>32</sup>  
543 A  $p < 0.05$  was considered significant and shown in bold.

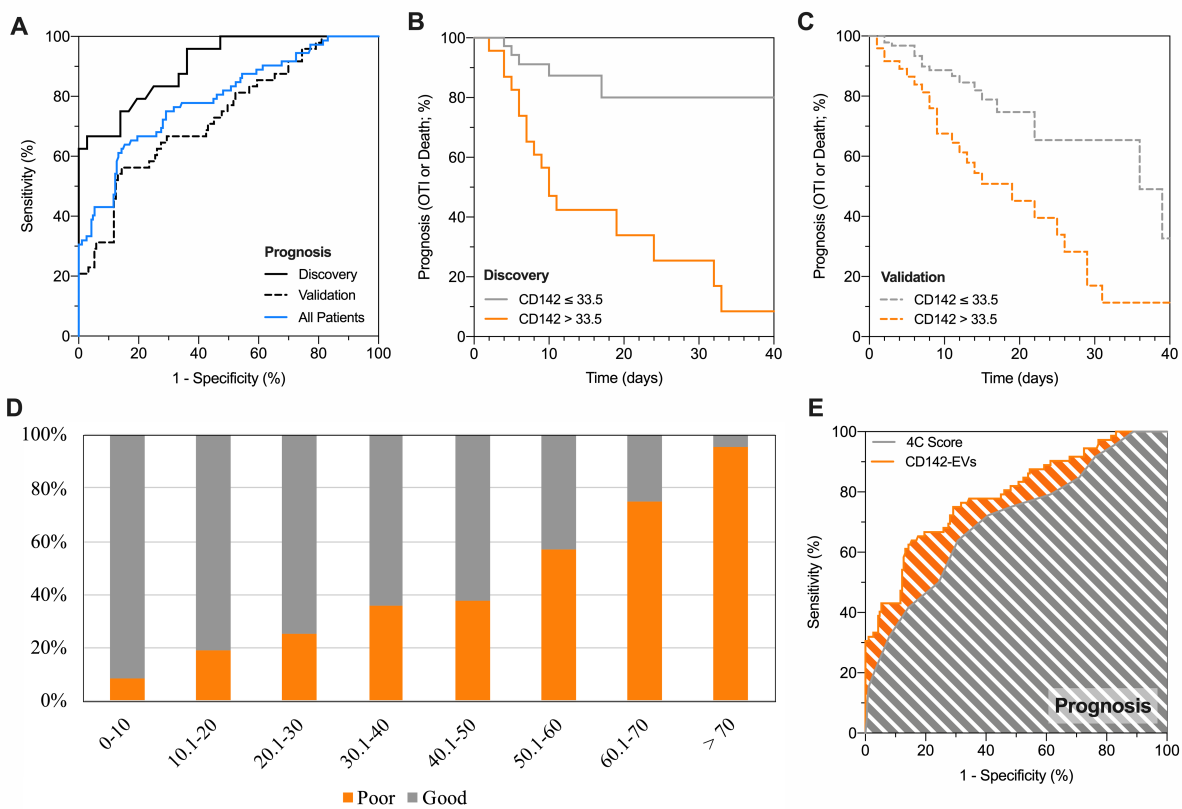


544

545 **Legend to Figure 1. EV surface antigens associated to patient outcome**

546 Profiling of EV surface antigens in patients admitted to hospital for SARS-CoV2 infection  
 547 and pneumonia in the discovery cohort (n=60). Patients were stratified for outcome (good  
 548 prognosis, grey, vs. poor prognosis, orange; a poor prognosis is defined as need of  
 549 orotracheal intubation or death) and mortality. Median fluorescence intensity (MFI) was  
 550 analyzed after normalization by the average MFI of CD9-CD63-CD81 (normalized MFI;  
 551 nMFI, %). **(A)** Expression levels of EV surface antigens differentially expressed in patients  
 552 with good vs. poor prognosis; **(B)** Association of EV surface antigens with patient outcome

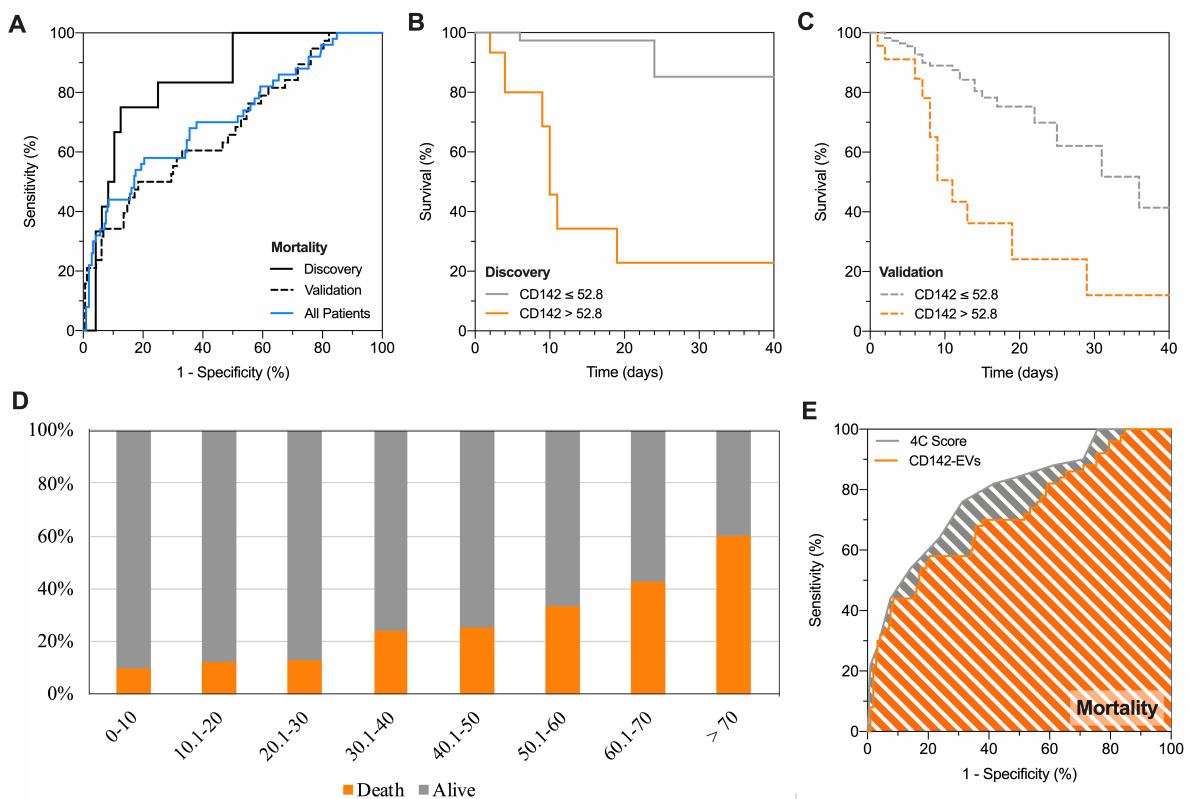
553 (good vs. poor prognosis; a poor prognosis is defined as need of orotracheal intubation,  
 554 OTI, or death). Hazard ratios (HRs) are shown together with their 95% confidence intervals.  
 555 **(C)** ROC curves for EV surface antigens discriminating patients according to prognosis. **(D)**  
 556 Expression levels of EV surface antigens differentially expressed in patients stratified for  
 557 mortality. **(E)** Association of EV surface antigens with mortality. Hazard ratios (HRs) are  
 558 shown together with their 95% confidence intervals. **(F)** ROC curves for EV surface antigens  
 559 discriminating patients according to mortality. Statistics is reported in Online Tables 4-6-8-  
 560 9-10. \*  $p < 0.01$ ; \*\* $p < 0.01$ ; \*\*\* $p < 0.001$ .  
 561



562  
 563 **Legend to Figure 2. CD142-EV to predict patient prognosis**

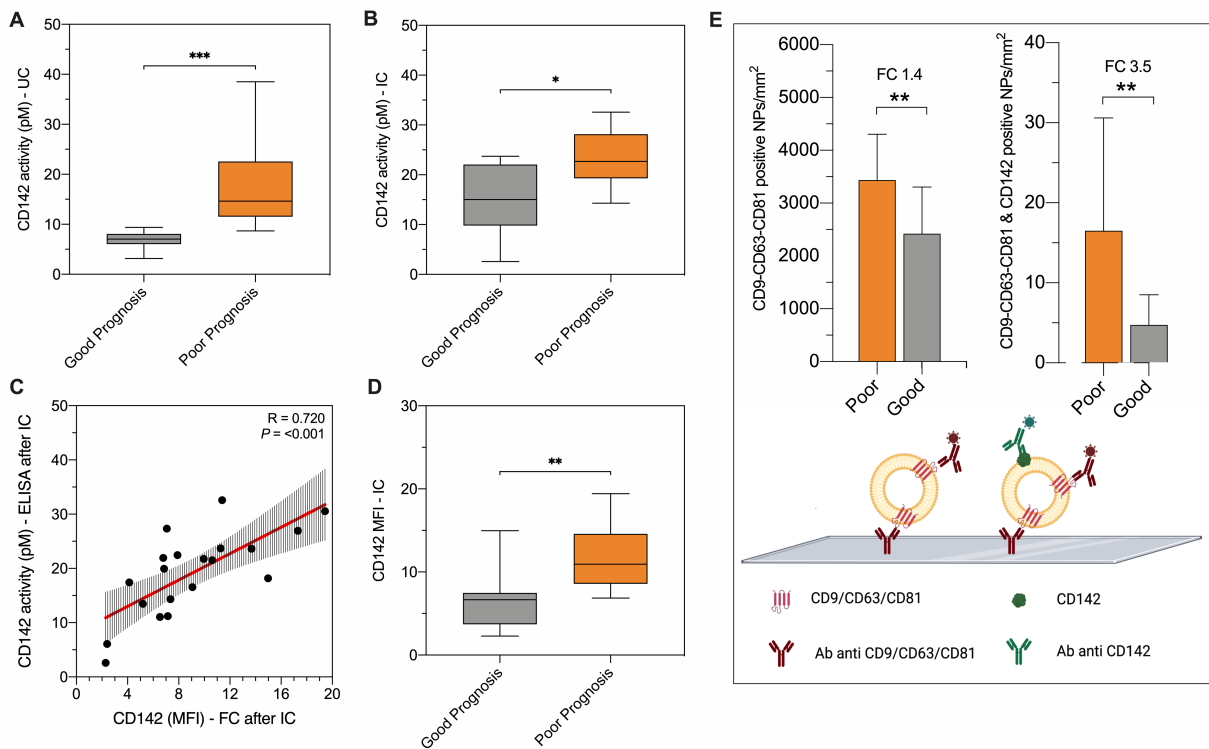
564 Performance of CD142 expressed on EV surface (CD142-EV) to predict outcome (poor  
 565 prognosis vs. good prognosis) in patients with SARS-CoV2 infection and pneumonia  
 566 (Discovery cohort, n=60; Validation cohort, n= 201; All patients, n=261); a poor prognosis is  
 567 defined as need of orotracheal intubation or death. Median fluorescence intensity (MFI) was  
 568 analyzed after normalization by the average MFI of CD9-CD63-CD81 (normalized MFI;  
 569 nMFI, %) for each EV antigen. **(A)** ROC curves showing performance of CD142-EV to  
 570 predict patient prognosis: AUC at discovery = 0.906 (0.833-0.979); AUC at validation = 0.736  
 571 (0.654-0.818); AUC in all patients = 0.792 (0.728-0.855). **(B)** Kaplan-Meier curves for  
 572 CD142-EV; the cut-off (nMFI = 33.5%) to discriminate patient outcome (good vs. poor

573 prognosis; discovery cohort) was defined by analysis of ROC curves. HR (log-rank) = 4.75  
 574 (95% CI 2.09-10.81). (C) Kaplan-Meier curves for CD142-EV; the cut-off (nMFI = 33.5%) to  
 575 discriminate patient outcome (good vs. poor prognosis; validation cohort) was defined by  
 576 analysis of ROC curves. HR (log-rank) = 2.22 (95% CI 1.23-3.99). (D) Stratification of  
 577 patients according to levels of expression of CD142 on EV surface and patient prognosis  
 578 (good prognosis, grey; poor prognosis, orange) on the combined discovery and validation  
 579 cohorts. (E) ROC curve analysis: prediction of patient prognosis; CD142-EV vs. 4C Score<sup>5</sup>.  
 580 Statistics is reported in Online Tables 11-12-13.  
 581



582  
 583 **Legend to Figure 3. CD142-EV to predict patient prognosis and mortality**  
 584 Performance of CD142 expressed on EV surface (CD142-EV) to predict mortality (death vs.  
 585 alive) in patients with SARS-CoV2 infection and pneumonia (Discovery cohort, n=60;  
 586 Validation cohort, n= 201; All patients, n=261). Median fluorescence intensity (MFI) was  
 587 analyzed after normalization by the average MFI of CD9-CD63-CD81 (normalized MFI;  
 588 nMFI, %) for each EV antigen. (A) ROC curves showing performance of CD142-EV to  
 589 predict mortality: AUC at discovery = 0.842 (0.727-0.957); AUC at validation = 0.682 (0.585-  
 590 0.779); AUC in all patients = 0.714 (0.630-0.798). (B) Kaplan-Meier survival curves for  
 591 CD142-EV; the cut-off (nMFI = 52.8%) to predict patient mortality (discovery cohort) was

592 defined by analysis of ROC curves. HR (log-rank) = 11.30 (95% CI 2.82-45.34). (C) Kaplan-  
 593 Meier survival curves for CD142-EV; the cut-off (nMFI = 52.8%) to predict patient mortality  
 594 (validation cohort) was defined by analysis of ROC curves. HR (log-rank) = 3.37 (95% CI  
 595 1.27-8.93). (D) Stratification of patients according to mortality (alive, grey; death, orange).  
 596 (E) ROC curve analysis: prediction of mortality; CD142-EV vs. 4C Score<sup>5</sup>. Statistics is  
 597 reported in Online Tables 11-12-13.  
 598



599

600 **Legend to Figure 4. Experimental validation with different techniques**

601 The discriminant performance of CD142-EV was experimentally validated by different  
 602 techniques in patients with SARS-CoV2 infection: good prognosis (grey; n=10) vs. poor  
 603 prognosis (orange; n=10). (A-B) CD142 activity per particle measured by ELISA (pM per  
 604 10<sup>9</sup> particles), after EV isolation by ultracentrifugation (UC) or immunocapture (IC using  
 605 beads covered by antibodies against CD9-CD63-CD81). (C) Correlation between CD142  
 606 activity per particle (pM) and CD142 MFI at flow cytometry after IC. (D) CD142-EV MFI after  
 607 IC (direct staining after immuno-capture, using beads covered by antibodies against CD9-  
 608 CD63-CD81). (E) Colocalization of tetraspanins (CD9-CD63-CD81) and CD142 was  
 609 assessed by ExoView® R100 Analyzer. Data are reported for mean number of  
 610 nanoparticles (NPs) per mm<sup>2</sup> for vesicles labelled with fluorochrome-conjugated antibodies  
 611 against CD9-CD63-CD81 and for the double positive for CD9-CD63-CD81 and CD142.